sible that as lithium is being removed from the structure the anti-site defect concentration is increased, blocking the lithium diffusion paths and making subsequent lithium intercalation/deintercalation more difficult or even impossible.[40,41] This may also be a source of irreversibility in the electrochemical reactions.

Conclusion

We have discovered the first metallic, layered lithium ternary nitride, $LiMoN_2$. This is the first reported synthesis of a ternary nitride from molecular ($Li_2Mo(N^tBu)_4$) or oxide (Li_2MoO_4) precursors. The structure has cation anti-site defects at the level of 15%. Up to 64% of the lithium can be chemically deintercalated and reintercalated. However, in electrochemical cells little reversibility is seen. The high degree of covalency in this material produces the shortest N-N contacts of any known nitride, and may result in a weak N-N interaction. Recent electronic structure calculations on the *hypothetical ordered structure* indicate a signifiant amount of nitrogen contribution to the wave functions at the Fermi level.[37] This has prompted us to search for alternative synthetic conditions and routes to achieve this ordered state.

The chemistry and properties of the lithium intercalated dichalcogenide layered compounds $LiMX_2$ (X = S, Se; M = IVb, Vb, VIb transition metals)[42,43] and the layered oxides[21] have been known and studied for over 25 years. Long term interest in these materials is due in part to their potential use in recyclable lithium batteries[44] and as catalysts. The discovery of $LiMoN_2$ affords a rare opportunity to compare the structure and properties of a material intermediate to the analogous layered ternary chalcogenides and oxides. The structure is similar to that found in the chalcogenides and oxides, and in general the physical and chemical properties can be rationalized on the basis of the models developed for those materials. The major difference is in the degree of covalency in the metal-nitrogen bonding, being less than in chalcogenides and more than in the oxides, which does have subtle affects on the physical and electronic structure.[37]

Acknowledgment. We are grateful to the Office of Naval Research for its generous support of our nitride work and the Department of Education Fellowship supporting S.H.E. We are are also grateful to Mike Rutzke in the Department of Fruit and Vegetables at Cornell University for assistance in the PES analysis, Daccai Xie at the H4S high flux beam reactor at BNL for collecting the neutron diffraction data and Joe Hriljac for the synchrotron X-ray diffraction data collection on beamline X-7A at NSLS supported by the Division of Materials Science (DOE) under contract DE-AC02-76CH0001 to D. E. Cox.

---

(40) Murphy, D. W. *NATO Conf. Ser. E* **1985**, *101*, 181.
(41) Sandre, E.; Brec, R.; Rouxel, J. *J. Solid State Chem.* **1990**, *88*, 269.
(42) Whittingham, M. S. *Prog. Solid State Chem.* **1978**, *12*, 41.
(43) Rouxel, J. *In Physics and Chemistry of Compounds with Layered Structures*; Levy F., Ed.; Reidel: Dordrecht, Netherlands, 1979; p 201.
(44) Whittingham, M. S. *J. Electrochem. Soc.* **1976**, *123*, 315.

Ammonia-Induced Pyrolytic Conversion of a Vinylic Polysilane to Silicon Nitride

Wayde R. Schmidt,[*,†] Paul S. Marchetti,[‡] Leonard V. Interrante,[*,§]
William J. Hurley, Jr.,[†] Russell H. Lewis,[‡] Robert H. Doremus,[†] and
Gary E. Maciel[‡]

*Department of Materials Engineering, Rensselaer Polytechnic Institute,
Troy, New York, 12180-3590; Department of Chemistry, Colorado State University,
Fort Collins, Colorado 80523; and Department of Chemistry, Rensselaer Polytechnic Institute,
Troy, New York, 12180-3590*

Received April 9, 1992. Revised Manuscript Received June 5, 1992

The decomposition of a vinylic polysilane precursor to Si_3N_4 was examined during thermolysis of the polymer from 25 to 1000 °C in anhydrous NH_3. The polymer cross-links primarily through pendant vinyl groups below 300 °C in NH_3 into a rigid, highly porous solid. Ammonia provides the source of N, which is incorporated into the originally N-free polysilane, and acts to quench free radicals which are formed during decomposition of the polymer. Significant incorporation of N into the polymer, with associated loss of C, occurs between 300 and 650 °C, as shown by infrared spectroscopy, elemental analysis, and ^{13}C and ^{29}Si solid-state MAS NMR spectroscopy. The polymer converts to a largely amorphous (by X-ray powder diffraction) Si_3N_4, containing isolated nanometer-sized crystals of α-Si_3N_4 and less than 2% C, on heating to 1000 °C. Further crystallization, grain growth, and reduction in C and H content occur upon additional heating to 1600 °C in N_2.

Introduction

Silicon nitride is an advanced structural ceramic and dielectric with applications in high-temperature environments and in electronics. Si_3N_4 powders are commonly prepared by the following methods: (1) direct nitridation of silicon from 1100 to 1400 °C;[1,2] (2) carbothermal re-

---

[†] Department of Materials Engineering, RPI.
[‡] Colorado State University.
[§] Department of Chemistry, RPI.

(1) Messier, D. R.; Croft, W. J. In *Preparation and Properties of Solid State Materials*; Wilcox, W. R., Ed.; Marcel Dekker: New York, 1982; Vol. 7, Chapter 2.

0897-4756/92/2804-0937$03.00/0 © 1992 American Chemical Society

duction and nitridation of SiO_2[2,3] or rice husks;[4] (3) vapor-phase or liquid-phase reactions between silane or chlorinated silanes and NH_3, followed by treatment at high temperatures in N_2 or NH_3.[5-7]

The development of organometallic precursors to silicon nitride is currently an area of growing interest due to the processing advantages afforded by soluble or melt-processible polymers. Pyrolysis of polysilazanes, $-[R_2SiNR']_x-$, poly(carbosilanes), $-[R_2SiCR_2']_x-$, and polysilanes, $-[R_2SiSiR_2']_x-$ in N_2 or NH_3 to form Si_3N_4/SiC composites or Si_3N_4 is well documented.[8-22] These papers report primarily on the synthesis of the ceramic precursors and characterization of ceramic end products, with little attention devoted to the isolation and characterization of intermediate pyrolysis products or the identification of chemical reactions associated with decomposition of these polymers.

Polysilazanes have been the polymers most studied as precursors to silicon nitride or silicon carbonitride. Arkles[8] pyrolyzed oligomeric polysilazanes in N_2 to 800 °C to form mixtures of Si_3N_4 and SiC as suggested by elemental analysis stoichiometries. Seyferth and co-workers[9] have reported the use of polysilazane oils and solids obtained from the ammonolysis of mixtures of chlorosilanes and alkyl-substituted chlorosilanes as Si_xN_y precursors. These researchers recently described studies which examined the conversion chemistry of such polysilazanes.[9i] Mutin, Corriu, and co-workers used similar oligosilazane compounds that incorporated specific chemical functionality to provide thermal cross-linking prior to pyrolysis.[21] They used thermal analysis coupled with mass spectrometry to investigate the effect of silazane functionality on the resulting ceramic. Blum, Laine, and co-workers have prepared oligo- and polysilazanes by the transition-metal-catalyzed dehydrocoupling of Si–H and N–H bonds[10-15] and characterized the pyrolysis products with thermal analysis, electron microscopy, and mass spectrometry[13,14] techniques.

Few researchers have addressed the role that NH_3 plays during the decomposition of C-containing polymer precursors to Si_3N_4. Okamura and co-workers[18] prepared Si–N–C fibers from the nitridation of a poly(carbosilane) cured by electron irradiation and heated in NH_3. Burns and others[19] investigated the role of NH_3 during the pyrolysis of thermally cross-linked poly(carbosilanes), chlorinated polysilanes, and polysilazane precursors and the effect of chain substituents on the efficacy of carbon removal. They note that conversion of the polymers to Si_3N_4 involves both the removal of carbon and the formation of residue containing Si–N bonding and suggest that $^{\bullet}NH_2$ radicals are generated during decomposition of NH_3. Durham and co-workers carbothermally reduced SiO_2 in the presence of excess carbon at 1300–1400 °C in an NH_3 atmosphere to produce predominantly α-Si_3N_4.[3] They compared the system $SiO_2/C/NH_3$ with that of $SiO_2/C/N_2$ and found that the use of NH_3 produced greater reaction rates from 1350 to 1400 °C because it dissociated to "active forms of hydrogen and nitrogen". Corriu and co-workers have recently reported on the pyrolysis of Yajima's poly(carbosilane) in both argon and ammonia using thermal analysis coupled with mass spectrometry.[22] These researchers propose that amination of the poly(carbosilane) and carbon removal start well below the thermal decomposition of ammonia, involving nucleophilic substitution on silicon by ammonia.

The purpose of the present study was to gain information on the role of NH_3 during the decomposition of a vinylic polysilane (VPS) which had previously been employed as a precursor to SiC.[23] We have recently reported a detailed investigation of the conversion chemistry of this precursor to C-rich SiC in N_2 to 1000 °C[24] and have shown

---

[2] Mori, M.; Inoue, H.; Ochiai, T. Preparation of Silicon Nitride Powder from Silica. In *Progress in Nitrogen Ceramics*; Riley, F. L., Ed.; Martinus Nijhoff: The Hague, 1983; pp 149–55.

[3] Durham, B. G.; Murtha, M. J.; Burnet, G. *Adv. Ceram. Mater.* **1988**, *3* (1), 45–58.

[4] Rahman, I. A.; Riley, F. L. *J. Eur. Ceram. Soc.* **1989**, *5*, 11–22.

[5] Hirai, T.; Hayashi, S. *J. Am. Ceram. Soc.* **1981**, *64*, C88–89.

[6] Mazdiyasni, K. S.; Cooke, C. M. *J. Am. Ceram. Soc.* **1973**, *56*, 628–33.

[7] (a) Segal, D. *Chemical Synthesis of Advanced Ceramic Materials*; Cambridge University Press: New York, 1989; p 90. (b) Crosbie, G. M. *Ceram. Eng. Sci. Proc.* **1986**, *7*, 1144.

[8] Arkles, B. *J. Electrochem. Soc.* **1986**, *133*, 233.

[9] (a) Seyferth, D.; Wiseman, G. H.; Prud'homme, C. Silicon-Nitrogen Polymers and Ceramics Derived from Reactions of Dichlorosilane, H_2SiCl_2. In *Emergent Process Methods for High-Technology Ceramics*; Davis, R. F., Palmour, H. III, Porter, R. L., Eds.; Plenum Press: New York, 1984; Materials Science Research, Vol. 17. (b) Seyferth, D.; Wiseman, G. H. *Polym. Prepr. (ACS Div. Polym. Chem.)* **1984**, *25* (1), 10. (c) Seyferth, D.; Wiseman, G. H.; Prud'homme, C. *J. Am. Ceram. Soc.* **1983**, *66*, C-13. (d) Seyferth, D.; Prud'homme, C.; Wiseman, G. H. U.S. Patent No. 4,397,828, Aug 1983. (e) Seyferth, D.; Wiseman, G. H. A Novel Polymeric Organosilazane Precursor to Si_3N_4/SiC Ceramics. In *Science of Ceramic Chemical Processing*; Hench, L. L., Ulrich, D. R., Eds.; Wiley: New York, 1986; pp 354–362. (f) Seyferth, D.; Wiseman, G. H. In *Ultrastructure Processing of Ceramics, Glasses, and Composites*; Hench, L. L., Ulrich, D. R., Eds.; Wiley: New York, 1984; pp 265–271. (g) Seyferth, D.; Wiseman, G. H.; Schwark, J. M.; Yu, Y.-F.; Poutasse, C. A. Chapt. 11 In *Inorganic and Organometallic Polymers*; ACS Symp. Series 360; Zeldin, M., Wynne, K. J., Allcock, H. K., Eds.; American Chemical Society: Washington, DC, 1988; p 143. (h) Seyferth, D.; Wiseman, G. H.; Poutasse, C. A.; Schwark, J. M.; Yu, Y.-F. *Polym. Prepr. (ACS Div. Polym. Chem.)* **1987**, *28*, 389–92. (i) Han, H. N.; Lindquist, D. A.; Haggerty, J. S.; Seyferth, D. *Chem. Mater.* **1992**, *4*, 705.

[10] Laine, R. M.; Blum, Y. D.; Tse, D.; Glaser, R. Ch. 10, In *Inorganic and Organometallic Polymers*; ACS Symp. Series 360; Zeldin, M., Wynne, K. J., Allcock, H. K., Eds.; Washington, DC, 1988; p 124.

[11] Blum, Y. D.; Laine, R. M.; Schwartz, K. B.; Rowcliffe, D. J.; Bening, R. C.; Cotts, D. B. *Mater. Res. Soc. Symp. Proc.* **1986**, *73*, 389.

[12] Schwartz, K. B.; Blum, Y. D. *Mater. Res. Soc. Symp. Proc.* **1988**, *121*, 483.

[13] Schwartz, K. B.; Rowcliffe, D. J.; Blum, Y. D.; Laine, R. M. *Mater. Res. Soc. Symp. Proc.* **1986**, *73*, 407.

[14] Blum, Y. D.; Schwartz, K. B.; Laine, R. M. *J. Mater. Sci.* **1989**, *24*, 1707–18.

[15] Laine, R. M.; Blum, Y. D.; Hamlin, R. D.; Chow, A. In *Ultrastructure Processing of Advanced Ceramics*; Mackenzie, J. D., Ulrich, D. R., Eds.; Wiley: New York, 1988; Chapter 58, p 761.

[16] Baney, R. H. *Polym. Prep. (ACS Div. Polym. Chem.)* **1984**, *25*, 2.

[17] Schwab, S. T.; Blahchard-Ardid, C. R. *Mater. Res. Soc. Symp. Proc.* **1988**, *121*, 581.

[18] (a) Okamura, K.; Sato, M.; Hasegawa, Y. *Ceram. Int.* **1987**, *13*, 55–61. (b) Taki, T.; Inui, M.; Okamura, K.; Sato, M. *J. Mater. Sci. Lett.* **1989**, *8*, 1119–1121.

[19] (a) Burns, G. T.; Chandra, G. *J. Am. Ceram. Soc.* **1989**, *72*, 333–37. (b) Burns, G. T.; Angelotti, T. P.; Hanneman, L. F.; Chandra, G.; Moore, J. A. *J. Mater. Sci.* **1987**, *22*, 2609–14.

[20] Hanna, S. B.; Mansour, N. A. L.; Taha, A. S.; Abd Allah, A. M. S. *Brit. Ceram. Trans. J.* **1985**, *84*, 18–21.

[21] (a) Choong Kwet Yive, N. S.; Corriu, R. J. P.; Leclercq, D.; Mutin, P. H.; Vioux, A. *Chem. Mater.* **1992**, *4*, 141–146. (b) Choong Kwet Yive, N. S.; Corriu, R. J. P.; Leclercq, D.; Mutin, P. H.; Vioux, A. *New J. Chem.* **1991**, *15*, 85.

[22] Corriu, R. J. P.; Leclercq, D.; Mutin, P. H.; Vioux, A. *Chem. Mater.* **1992**, *4*, 711.

[23] (a) Schilling, C. L., Jr. *Brit. Polym. J.* **1986**, *18*, 355. (b) Schilling, C. L., Jr.; Wesson, J. P.; Williams, T. C. *J. Am. Ceram. Soc. Bull.* **1983**, *62*, 912. (c) Schilling, C. L., Jr.; Williams, T. C. *Polym. Prepr. (ACS Div. Polym. Chem.)* **1984**, *25*, 1. (d) Schilling, C. L., Jr. Tech. Report No. 83-3 on ONR Contract N00014-81-C-0682; Sept 1983. (e) Schilling, C. L., Jr.; Wesson, J. P.; Williams, T. C. *J. Polym. Sci., Polym. Symp.* **1983**, *70*, 121. (f) Schilling, C. L., Jr.; Williams, T. C.; Wesson, J. P. U.S. Patent No. 4,414,403, Nov 1983. (g) Schilling, C. L., Jr.; Williams, T. C. U.S. Patent No. 4,472,591, Sept 1984.

Table I. Heating Schedules Used during the Pyrolysis of VPS in Flowing NH_3 and the Morphology of the Isolated Solids

sample	heating schedule	sample appearance following heating
VPS	none	translucent, viscous liquid
250A	25 to 250 °C in 1 h; 250 °C hold 10 h; furnace cool	yellow glassy solid, extensive porosity
400A	25 to 250 °C in 1 h; 250 °C hold 3 h; 250 to 400 °C in 1 h; 400 °C hold 10 h; furnace cool	brown glassy solid, extensive porosity
650A	25 to 250 °C in 2 h; 250 °C hold 3 h; 250 to 650 °C in 3 h; 650 °C hold 10 h; furnace cool	black glassy solid, extensive porosity
1000A	25 to 250 °C in 2 h; 250 °C hold 3 h; 250 to 2000 °C in 6 h; 1000 °C hold 10–15 h; furnace cool	tan glassy solid, extensive porosity
1600A	sample 1000A, ground; 25 to 1600 °C in 4 h in N_2; 1600 °C hold 4 h in N_2; furnace cool in N_2	off-white solid

that this same precursor decomposes in NH_3 to high-purity, high-surface-area Si_3N_4.[25,26] We report here the results of a study of the pyrolysis of VPS to 1000 °C in NH_3 and a comparison with those reported previously during pyrolysis in N_2.[24]

Experimental Section

Materials. VPS was purchased from Union Carbide Corp., Tarrytown, NY (Y-12044 Vinylic Polysilane), stored in a N_2-filled glovebox at −20 °C in a sealed opaque bottle prior to use, and pyrolyzed without further treatment. We have determined that VPS contains at least five different types of Si bonding environments in the polysilane chain and has the approximate formula $[[(SiMe_3)_{0.32}[Si(CH{=}CH_2)Me]_{0.35}[Si(H)Me]_{0.18}[SiMe_2]_{0.07}[CH_2SiMe_3]_{0.08}]_n$, where Me represents a $-CH_3$ group.[24] N_2 was purified as previously reported.[24] Anhydrous NH_3 (Scott Specialty Gases) was further dried in-line over a mixed bed of 3-Å molecular sieves and predried flaked KOH. This NH_3 was used for all pyrolysis experiments.

Analysis. Transmission infrared spectra (TGS detector, 4-cm^{-1} resolution) were recorded in air using a Perkin-Elmer 1850 FTIR spectrophotometer coupled with a Deltech dry air purge assembly. Liquid VPS samples were prepared in N_2 as smears between KBr windows. Preceramic and ceramic solids were diluted with KBr (ca. 20:1, International Crystal Laboratories) and pressed as transparent disks. Samples for IR study were transferred in sealed, N_2-filled bags to minimize exposure to air and moisture; samples with high surface area were found to partially oxidize/hydrolyze on long exposure in air. Elemental analyses were performed by Galbraith Laboratories, Inc., Knoxville, TN, and Leco Corporation, St. Joseph, MI. Thermogravimetric analyses of VPS were performed in flowing NH_3 (0.05–0.1 standard cubic feet/hour (scfh)) with a Perkin-Elmer 7 Series thermal analysis system at heating rates of 5–20 °C/min to 1000 °C. Typical sample sizes ranged from 10 to 25 mg.

NMR Methods. Solid-state spectra were obtained using either a Bruker MSL 200 or a converted Nicolet NT-150 spectrometer. Measurements on the MSL 200 utilized a Doty magic angle spinning (MAS) probe (Doty Scientific, Inc.) and 7-mm-o.d. ceramic rotors. The NT-150 spectrometer utilized an in-house built MAS probe with a cylindrical rotor system with rotors machined from Delrin (^{29}Si) or Kel-F (^{13}C).[27] All spectra were obtained in natural abundance. Silicon-29 spectra were acquired at observe frequencies of 39.763 and 29.810 MHz using single pulse excitation (30° pulse) and 300-s relaxation delay, except in the case of neat VPS, where a 15-s delay was used. A total of 128 transients was accumulated and 50-Hz line broadening was applied before Fourier transformation. Carbon-13 spectra were acquired at 50.327 and 37.735 MHz using a single-pulse excitation (30° pulse) and a 10-s relaxation delay. Between 1000 and 2000 transients were accumulated before Fourier transformation using 50-Hz line broadening. Proton decoupling was carried out during data acquisition on all samples. All chemical shifts were referenced to tetramethylsilane (TMS).

ESR Methods. Spin counting was carried out on a Bruker ESP300 X-band (9.5 GHz) ESR spectrometer. Spin densities, given in number of spins per gram of sample, were determined by comparing integrated signal intensities of the sample with that of a standard having a known spin density (polystyrene doped with a known concentration of α,γ-bisdiphenylene-β-phenylallyl).[28] In addition to the spin count, the dynamic nuclear polarization (DNP)[27] experiment was carried out on a home-built 1.4-T spectrometer on sample 650A from this study and sample 650N from our previous work.[24] Enhancement curves were determined for each sample by measuring signal intensity as a function of microwave frequency.

Pyrolysis of VPS. On the basis of temperatures where significant weight losses occurred during TGA experiments, bulk portions of VPS (5–10 g) were heated in NH_3 according to the schedules reported in Table I. These portions were poured into molybdenum foil boats and loaded into an elastomer-ring-sealed fused silica furnace tube which was sealed in the glovebox, under N_2, by clamping. The tube was equipped with gas inlet and outlet valves. The loaded tube was placed into a programmable furnace (CM Furnaces 1000 Series) and flushed with NH_3 for about 10 min prior to heating. All pyrolyses were conducted at 1 atm in flowing (0.3–0.5 scfh) NH_3. Volatile decomposition products were either sampled directly at the outlet, through an in-line septum via syringe, or collected in liquid N_2 traps, which were connected to the furnace outlet tube. Collected decomposition products were transferred and separated on a vacuum line by trap-to-trap distillation and subsequently analyzed by gas chromatography (GC, Shimadzu GC-9A) or coupled GC/FTIR (Varian 3700 GC/Perkin-Elmer 1850 FTIR) techniques. The GC/FTIR combined technique was operated in a dual-detection mode (GC-TCD detector, FTIR-MCT detector). Hydrocarbons and silanes were separated on an Alltech VZ-10 column (6 ft, 0.085-in.-i.d., 60–80 mesh range), while the presence of amines was investigated using a Chromosorb-103 column (6 ft, 0.085-in.-i.d., 80–100 mesh range).

Immediately following pyrolysis and cooling, the furnace tube was flushed with N_2 and unloaded in the glovebox. Solid products were stored and dry-ground to uniform fine powders in N_2 prior to FTIR, NMR, XRD, ESR, and elemental analyses. Experiments requiring temperatures above 1000 °C were performed using a custom-built 2-chamber, molybdenum wire-coiled furnace,[25] through which purified N_2 flowed over the sample in the sealed inner chamber and H_2 flowed over the molybdenum heating element in the outer chamber.

Results

Weight Loss. We used the same VPS lot for initial thermogravimetric experiments and to prepare intermediate pyrolysis samples so that significant chemical differences resulting from the use of NH_3, relative to N_2, could be identified and a direct comparison could be made. Figure 1 shows a comparison of the measured weight losses during the decomposition of VPS in flowing NH_3 and N_2; samples were degassed under vacuum for 24 h prior to analysis, and experiments were performed using the identical heating rate of 5 °C/min. We noted that re-

---

[24] Schmidt, W. R.; Interrante, L. V.; Doremus, R. H.; Trout, T. K.; Marchetti, P. S.; Maciel, G. E. *Chem. Mater.* **1991**, *3*, 257.

[25] Schmidt, W. R.; Sukumar, V.; Hurley, W. J., Jr.; Garcia, R.; Doremus, R. H.; Interrante, L. V.; Renlund, G. M. *J. Am. Ceram. Soc.* **1990**, *73*, 2412.

[26] Hurley, W. J., Jr.; Interrante, L. V.; Garcia, R.; Doremus, R. H. *Ceram. Trans.* **1990**, *7*, 637.

[27] Wind, R. A.; Anthonio, F. E.; Duijvestijn, M. J.; Smidt, J.; Trommel, J.; DeVette, G. M. C. *J. Magn. Reson.* **1983**, *52*, 424.

[28] Poole, C. P., Jr. *Electron Spin Resonance*, 2nd ed.; Wiley: New York, 1983; p 443.

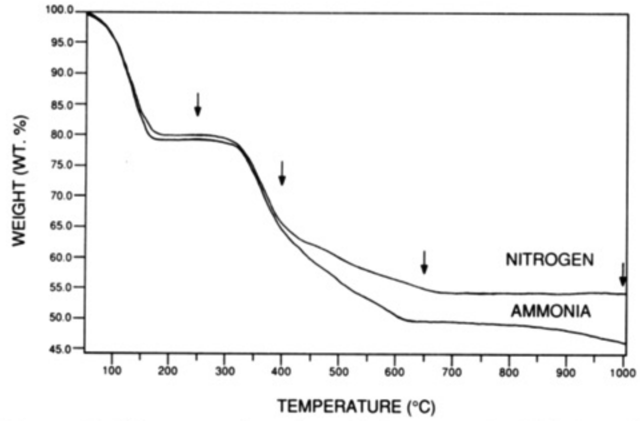

Figure 1. Thermogravimetric analysis curves for VPS heated in flowing NH_3 and N_2 (0.08–0.1 scfh) at 5 °C/min from 50 to 1000 °C. Sample sizes: N_2, 10.598 mg; NH_3, 12.161 mg. Arrows indicate final temperatures at which samples were heated in bulk pyrolysis experiments. See Table I and ref 24 for further experimental details.

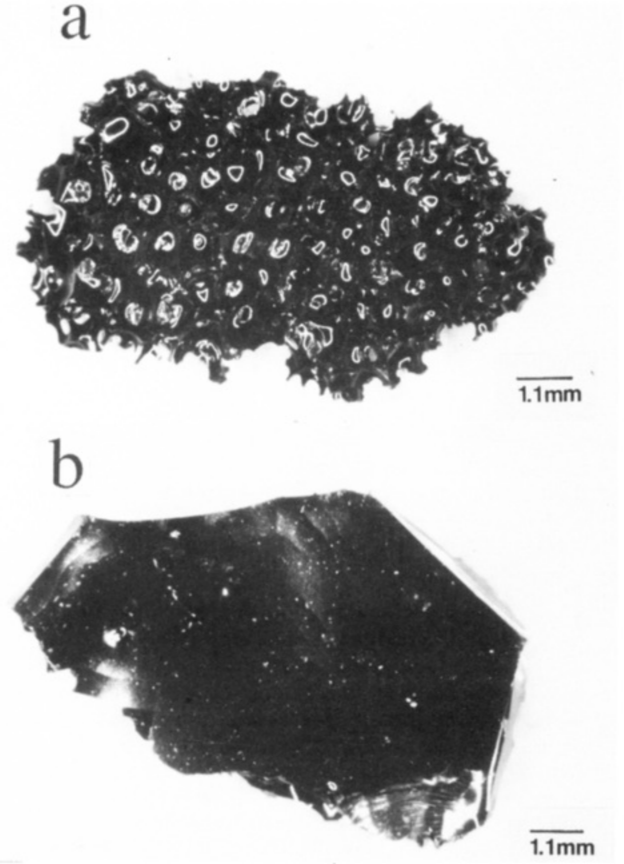

Figure 2. Optical micrographs showing the effect of pyrolysis atmosphere on sample morphology. VPS pyrolyzed in (a) NH_3, sample 650A, and (b) N_2, sample 650N.[24]

gardless of atmosphere, the magnitude of the initial weight loss decreased with an increase in the TGA heating rate. Both curves in Figure 1 exhibit a similar shape, although the overall weight loss is greater when NH_3 is used as the pyrolysis atmosphere. Three regions are apparent in the TGA curves: (1) 50–300 °C, where an initial 20–22% weight loss is seen followed by a plateau; (2) 300–650 °C, where an additional 25–35% weight loss occurs, accompanied by a decreasing slope of the TGA curve; (3) 650–1000 °C, where a further weight loss of 0–4% occurs. The char yield for the decomposition of VPS under NH_3 at 1000 °C is approximately 45%, which is significantly lower than the 55% yield seen for the N_2 curve. Based on the proposed formula presented in the Experimental Section, the theoretical yield for the conversion of the Si in VPS to Si_3N_4 is 69%.

Table II. Elemental Analyses (wt %) for Isolated Solids Obtained during the Pyrolysis of VPS in Flowing NH_3, According to Heating Schedules in Table I

sample	Si	N	C	H	O	atomic Si/N
VPS (as recd)	44.7	0.09[a]	46.3	8.88	0.06	247.8[a]
250A	34.6	0.31	39.8	7.75	7.36[b]	55.7
400A	40.4	3.90	43.2	8.03	4.11	5.16
650A	44.1	36.2	7.10	2.18	4.33	0.61
1000A	52.7	33.4	1.79	1.10	3.19	0.79
1600A	57.9	37.9	0.15	0.11	3.09	0.76
Si_3N_4 (theory)	60.1	39.9	0.00	0.00	0.00	0.75

[a] The polymer is not expected to contain N initially. [b] See ref 29.

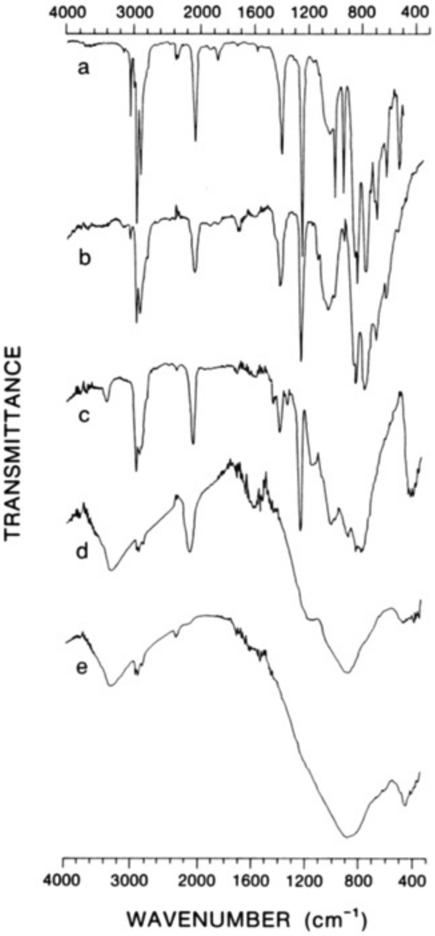

Figure 3. Transmission infrared spectra of isolated VPS samples heated in NH_3 according to schedules in Table I: (a) as-received VPS, (b) 250A, (c) 400A, (d) 650A, (e) 1000A. Atmospheric CO_2 is seen as two small bands between 2250 and 2400 cm^{-1}.

Regions of large or changing weight loss in the TGA curve were examined further in bulk pyrolysis experiments performed in flowing NH_3 (Table I) in an effort to characterize the chemistry and compositional changes which occur during the decomposition of VPS in the presence of NH_3. In these experiments, all isolated solid pyrolysis products exhibited extensive macroscopic porosity. Figure 2 shows the porous morphology of sample 650A, which is typical of all VPS samples that were pyrolyzed in NH_3, along with the smooth, nonporous appearance of sample 650N (the analogous sample obtained from pyrolysis of VPS at 650 °C in N_2[24]).

Elemental Analysis. The results for isolated samples are listed in Table II. With increasing pyrolysis temperature, the measured Si/N atomic ratio decreases from 55.7 for sample 250A[29] to a near stoichiometric value of 0.76 for sample 1600A, reflecting the incorporation of N into the polymer upon conversion to ceramic. The C content also decreases to a minimal level with increasing pyrolysis temperature. The largest change in both the gain in wt % N (32.3%) and the loss of wt % C (36.1%) occurs between 400 and 650 °C; both changes are associated with the temperature region of largest weight loss in the TGA curves (Figure 1).

Infrared Spectroscopy. The infrared spectra of solid samples isolated at intermediate temperatures during the decomposition of VPS in NH_3 monitor the conversion of VPS to Si_3N_4. Figure 3 shows a series of transmission infrared spectra of isolated preceramic and ceramic samples. As noted in our previous report,[24] the IR spectrum of liquid VPS (Figure 3a) exhibits peaks indicative of $CH{=}CH_2$ (3048, 1397 cm^{-1}), Si–H (2078 cm^{-1}), and C–H (2800–3000 cm^{-1}) functionalities. The spectrum of sample 250A (Figure 3b) exhibits virtually no vinyl functionality at 3048 cm^{-1}, and the C–H and Si–H bands have decreased in intensity and broadened. The intensity of the band attributed to the $Si{-}CH_2{-}Si$ deformation band (1046 cm^{-1}) in a "poly(carbosilane)" skeleton[24] is seen to increase with heating to 250 °C.

The spectrum of sample 400A (Figure 3c) shows essentially the same features as that of 250A; in addition, this spectrum exhibits a small band for N–H centered near 3390 cm^{-1},[30] which reflects the start of N incorporation into the polymer (Table II), as well as an increased relative intensity for the Si–H band, which we have previously associated with methylene (silylene) insertion during the decomposition of VPS.[24] The band at 1046 cm^{-1} in the spectrum of sample 400A has not increased significantly in intensity relative to the spectrum of sample 250A. The spectrum of sample 650A (Figure 3d) shows increased intensity for the N–H band, significantly reduced C–H stretch intensity, and a broadened Si–H stretching band relative to that for sample 400A.

The fingerprint region (1200–400 cm^{-1}) also shows a decreasing resolution of individual peaks as the pyrolysis temperature increases from 25 to 1000 °C. The spectrum of sample 1000A (Figure 3e) exhibits a relatively strong, broad N–H band, along with weak bands in the C–H and Si–H stretching regions. The broadened peak centered near 890 cm^{-1} is attributed to Si–N stretching vibrations in primarily amorphous Si_3N_4.[31-33] The significant intensity of the N–H stretching band is attributed to both residual N–H species and the moisture sensitivity of the high-surface-area amorphous material.[25] The IR transmission spectrum of sample 1600A (not shown) shows increased loss of N–H and C–H functionality and exhibits many sharp, resolved bands from 400–900 cm^{-1},[25] indicating crystallization to α-Si_3N_4.[31-33]

Mutsuddy has reported changes in the infrared spectrum of Yajima's poly(carbosilane) following humidification of the polymer for 7 days.[34] He noted that the presence of free water produced the infrared band between 1600 and 1680 cm^{-1} and that both absorbed and combined water produced a broad band between 3200 and 3600 cm^{-1}. Bands between 1020 and 1090 cm^{-1} were attributed to Si–O–C and Si–O–Si functionality. Humidification of pyrolyzed VPS samples is likely because of the high surface area of ground NH_3-pyrolyzed VPS samples[25] and the reactivity of residual N–H functionality in samples 400A, 650A, and 1000A (Figure 3). The differences between the IR spectra of polymeric species which contain N–H and those containing O–H functionality as well as polymers containing $Si{-}CH_2{-}Si$ or Si–O–C and/or Si–O–Si functionality are far more difficult to assess.

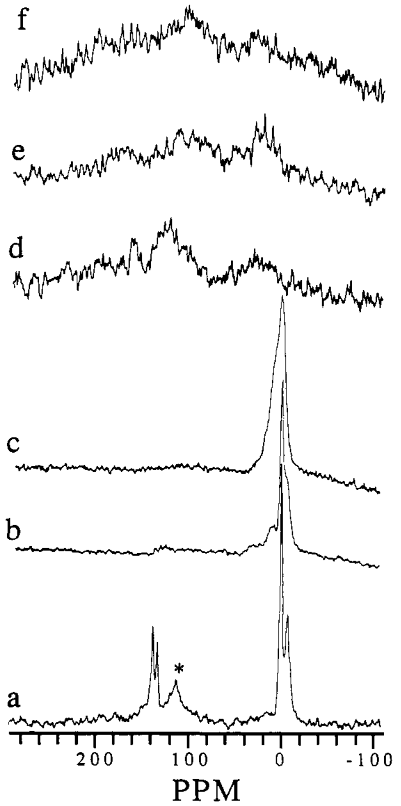

Figure 4. Solid-state ^{13}C MAS NMR spectra of isolated VPS samples heated in NH_3 according to schedules in Table I: (a) VPS, (b) 250A, (c) 400A, (d) 650A, (e) 1000A, (f) 1600A. Artifact peak at 112 ppm from the Teflon rotor insert is noted with an asterisk. Spectra d–f are plotted at increased vertical expansion compared to spectra a–c.

NMR Spectroscopy. The solid-state ^{13}C MAS spectra of VPS exhibits resonances for $R_3Si{-}{*}CH{=}{*}CH_2$ groups (131.9, 137.0 ppm),[24,35] $RSi{*}Me_3$ end groups (centered at −0.28 ppm),[24,35] and a combination of $R_2Si(H){*}Me$, $R_2Si(CH{=}CH_2){*}Me$, and $R_3SiSi({*}Me_2)SiR_3$ functional groups (centered at −7.74 ppm)[24,35] (Figure 4a). A small, broad peak (near 2 ppm) is attributed to residual $R_3Si{-}{*}CH_2{-}SiR_3$ functionality.[24,35] The Teflon insert is seen as an artifact peak at 112 ppm. Thermal cross-linking of VPS in NH_3 at 250 °C is seen as loss of the vinyl carbon resonances, a new peak near 11 ppm attributed to ethylene bridging between silicon atoms,[24] and loss of resolution of the peaks representing methyl functionality of H- and/or vinyl-substituted silicon/dimethylsilane units (Figure 4b). The solid-state ^{13}C MAS spectrum of sample 400A (Figure 4c) exhibits a single, broad peak centered near 5 ppm. At least two shoulders are apparent on the low shielding side

---

(29) The unusually high value for weight percent O in sample 250A may signal a higher nitrogen content for this sample than is indicated by the observed percent N value, with hydrolysis occurring prior to, or during, analysis.

(30) Colthup, N. B.; Daly, L. H.; Wiberley, S. E. *Introduction to Infrared and Raman Spectroscopy*, 3rd ed.; Academic Press: New York, 1990.

(31) Luongo, J. P. *Appl. Spectrosc.* **1984**, *38*, 195.

(32) Wada, N.; Solin, S. A.; Wong, J.; Prochazka, S. *J. Non.-Cryst. Solids* **1981**, *43*, 7.

(33) Trout, T. K.; Brinkman, F. E.; Bellama, J. M.; Faltynek, R. A. *J. Mater. Res.* **1989**, *4*, 399.

(34) Mutsuddy, B. C. *Ceram. Int.* **1987**, *13*, 41–53.

(35) (a) Williams, E. A. In *The Chemistry of Organic Silicon Compounds*; Patai, S., Rappoport, Z., Eds.; Wiley: New York, 1989; Chapter 6. (b) Williams, E. A. *Annu. Rep. NMR Spectrosc.* **1983**, *15*.

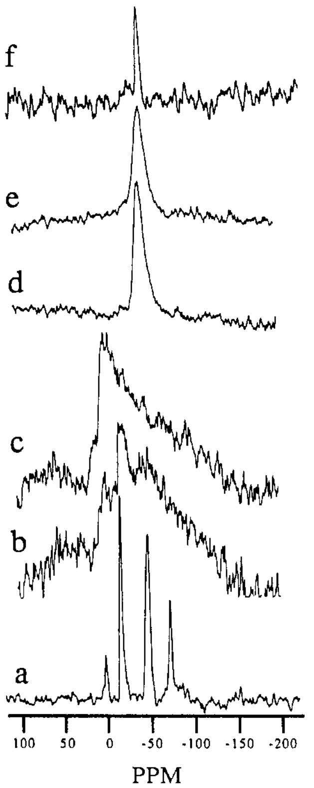

Figure 5. Solid-state ^{29}Si MAS NMR spectra of isolated VPS samples heated in NH_3 according to schedules in Table I: (a) VPS, (b) 250A, (c) 400A, (d) 650A, (e) 1000A, (f) 1600A.

of the peak. Solid-state ^{13}C MAS spectra of samples 650A, 1000A, and 1600A (Figure 4d–f) exhibit no sharp peaks, consistent with the low concentration of carbon indicated by elemental analysis. Very broad, poorly resolved bands can be discerned from 90–130 and 0–30 ppm and may be attributed to trace levels of graphitic[36] and carbidic[36–38] carbon, respectively.

The solid-state ^{29}Si MAS spectrum of VPS (Figure 5a) exhibits four major peaks which are attributed to R_3Si–$*Si(H)MeSiR_3$ (−72.1 ppm);[24,35] R_3Si–$*Si(Me_2)SiR_3$, R_3Si—$*Si(CH{=}CH_2)MeSiR_3$, and $-(*SiMe_2)_n-$ chains (−47.2 ppm);[24,35] R_3Si–$*SiMe_3$ (−16.4 ppm);[24,35] and $Me_3*SiCH_2Si(Me_2)SiR_3$ (1.31 ppm)[24,35] poly(carbosilane) residue. Heating in NH_3 to 250 °C significantly increases the number of different silicon environments, as seen by the very broad distribution of resonances from 25 to −125 ppm in the spectrum of sample 250A (Figure 5b). The spectrum of sample 400A (Figure 5c) consists of a similar broad distribution. Further heating in NH_3 from 650 to 1000 °C (Figures 5d,e) and in N_2 to 1600 °C (Figure 5f) causes the spectrum to sharpen considerably and shift to higher shielding for samples 650A (−44.8 ppm), 1000A (−46.5 ppm) and 1600A (−46.9 ppm). The observed peak widths and positions are consistent with those reported for amorphous and poorly crystalline α-Si_3N_4.[39,40] The two peaks which are expected for α-Si_3N_4 are not resolved,[40] although XRD indicates that less than 1.5% β-Si_3N_4 is present in sample 1600A.[25]

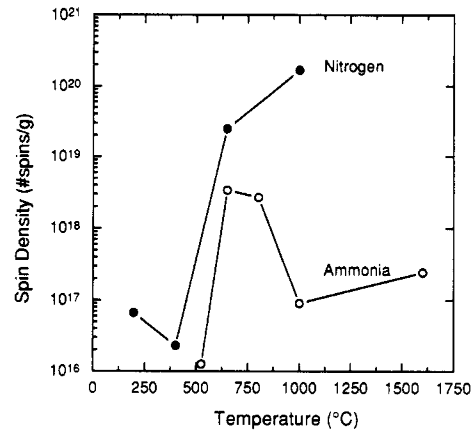

Figure 6. Spin densities as a function of temperature for solids isolated following the pyrolysis of VPS in NH_3 (○) and N_2 (●) according to heating schedules in Table I and ref 24.

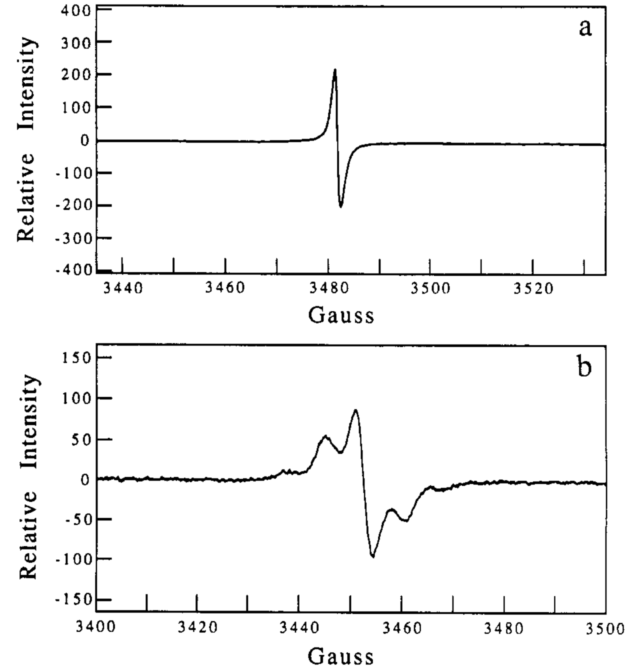

Figure 7. Representative ESR spectra of samples (a) 1000A and (b) 1600A from this study.

Gas Analysis. The types of gases collected and identified during the decomposition of VPS in NH_3 to 1000 °C were identical to those found during the N_2 decomposition experiments.[24] The major gaseous decomposition product was trimethylsilane; a significantly smaller amount of tetramethylsilane was found. Minor amounts of methane, ethane, ethylene and higher hydrocarbons were also identified. No gaseous amines were identified other than the NH_3 pyrolysis atmosphere; trace amounts may have been present, but these compounds were not separated from the NH_3 by the GC/FTIR or GC/MS methods employed. The presence of H_2 or HCN was not investigated.

ESR and DNP Analysis. The spin densities of the isolated solids are plotted versus pyrolysis temperature for both N_2 and NH_3 in Figure 6. For pyrolysis in N_2, the density of spins increases overall by 4 orders of magnitude from 6.7×10^{16} spins/g at 196 °C to 1.7×10^{20} spins/g at 1000 °C, while for pyrolysis in NH_3, spin density is not observed below 500 °C (below the detection limit of ca. 1×10^{16} spins/g) but increases to 3.4×10^{18} spins/g at 650 °C, followed by a decrease to 9.1×10^{16} spins/g at 1000 °C. The spin density of sample 1600A is slightly higher at 2.5×10^{17} spins/g. Typical behavior for carbon chars

---

(36) Haworth, D. T.; Wilkie, C. A. *J. Inorg. Nucl. Chem.* **1978**, *40*, 1689.

(37) Wagner, G. W.; Na, B.-K.; Vannice, M. A. *J. Phys. Chem.* **1989**, *93*, 5061.

(38) Carduner, K. R.; Shinozaki, S. S.; Rokosz, M. J.; Peters, C. R.; Whalen, T. J. *J. Am. Ceram. Soc.* **1990**, *73*, 2281.

(39) Carduner, K. R.; Carter, R. O., III; Milberg, M. E.; Crosbie, G. M. *Anal. Chem.* **1987**, *59*, 2794.

(40) Hatfield, G. R.; Carduner, K. R. *J. Mater. Sci.* **1989**, *24*, 4209.

Table III. Comparison of the ^{13}C Overhauser, Solid-State, and Thermal Mixing Effects for VPS Pyrolyzed to 650 °C in NH_3 (Sample 650A) and N_2 (Sample 650N[24])

effect	sample 650A enhancement	sample 650N enhancement
+solid state	1.0[a]	6.6[a]
+thermal mixing	0.0	1.2
Overhauser	−0.0	−1.2
−thermal mixing	−0.0	−3.4
−solid state	−1.0	−7.6

[a] These numbers represent the enhancement factors defined by $\eta = [I(\mu\omega)/I(0)] - 1$, where $I(\mu\omega)$ is the ^{13}C NMR intensity in the presence of microwave irradiation and $I(0)$ is the intensity in the absence of microwave irradiation.

is for the spin density to increase steadily for pyrolysis temperatures up to 600–800 °C, followed by a decrease as recombination sets in at higher temperatures.[41]

Even after the VPS samples had been converted to ceramics by heating to 1000 °C, the shape of each ESR spectrum is fairly typical of that of an organic free radical, showing no hyperfine structure (Figure 7a). The one exception to this is the ESR spectrum of sample 1600A, which shows at least three components as evident from the integral curve (Figure 7b).

In addition to the spin count, the dynamic nuclear polarization (DNP) experiment was carried out on samples 650A from this study and 650N from our previous study.[24] Enhancement curves were determined for each sample by measuring signal intensity as a function of microwave frequency. Figure 8 shows the effect of the DNP enhancement on the spectrum of sample 650N. The magnitudes of the Overhauser, solid-state, and thermal mixing effects[28] are compared for samples 650A and 650N in Table III.

Discussion

Our previous paper[24] detailed the decomposition chemistry of vinylic polysilane (VPS) in N_2 to form carbon-rich SiC. The present study compares the decomposition of the same batch of VPS polymer in NH_3 under identical thermal processing conditions to (1) investigate the effect of atmosphere type (e.g., reactive vs inert) on the decomposition of VPS and (2) ascertain the role(s) that NH_3 performs during the chemical conversion of VPS to ceramic silicon nitride, Si_3N_4.

Cross-Linking. The solid-state ^{13}C MAS NMR spectrum of sample 250A contains no peaks indicative of residual $R{-}CH{=}CH_2$ functionality, supporting the conversion of the vinyl groups to saturated hydrocarbon functionality, presumably due to radical-induced interchain oligomerization processes.[24] Some Si–H functionality is also lost during heating to 250 °C in NH_3 (as it is during cross-linking of VPS in N_2) as suggested by the lower relative intensity and the broadening of the IR band at 2078 cm^{-1} (Figure 3b) compared to the same band in the spectrum of unheated VPS (Figure 3a). This intensity loss may reflect hydrosilylation mechanisms, H-abstraction reactions, or elimination of H_2 gas as noted earlier.[24]

The infrared spectrum for sample 250A shows a somewhat increased level of $R_3Si{-}CH_2{-}SiR_3$ band intensity (1046 cm^{-1}), due to methylene insertion,[24] relative to the spectrum of as-received VPS. This result suggests the partial conversion of the polysilane to polycarbosilane prior to significant incorporation of N. These spectra also support the conclusion that VPS crosslinks in NH_3 by 250 °C in a manner much like that observed for this polymer in N_2, involving reaction of the pendant vinyl groups (3048 cm^{-1}).[24] We suggested earlier that this reaction was initiated by free radicals generated by the scission of the polysilane backbone[24] and that at higher temperatures, cleavage of Si–H, Si–C, and C–H bonds could contribute to the concentration of radical sites. Isolation of trimethylsilane as the primary gaseous decomposition product during pyrolysis in NH_3 or in N_2 is consistent with the view that cleavage of the Me_3Si- end groups to produce $Me_3Si^\bullet$ radicals occurs to a significant extent by 250 °C. An alternative process for the generation of trimethylsilane could involve the transfer of hydrogen from an adjacent Si–H group along with Si–Si bond breaking in a concerted fashion (eq 1):

$$Me_3Si{-}Si(H)RR' \rightarrow Me_3Si{-}H + {:}SiRR' \qquad (1)$$

however, on the basis of the measured rate data for $Me_2SiHSiHMe_2$,[42a] this reaction may not become very significant until about 400 °C. In addition to trimethylsilane, such a reaction would generate a silylene species which could insert into other Si–H bonds, C–H bonds,[42] or the N–H bonds of NH_3, producing in the latter case $RR'Si(H)NH_2$ species.

In related work, Brix and co-workers photolyzed hexamethyldisilane at 206 nm, in the presence and absence of radical and silene scavengers, and found two major decomposition routes; rupture of the Si–Si bond to yield trimethylsilyl radicals (71%) and the molecular elimination of 1,1′-dimethylsilene and trimethylsilane (27%).[43] Tokach and Koob did similar photolysis experiments on hexamethyldisilane at 147 nm and found three major decomposition pathways; Si–Si bond rupture to form trimethylsilyl radicals, molecular elimination of trimethylsilane, and Si–C bond rupture to form CH_3 radicals with quantum yields of 0.99, 0.26, and 0.52, respectively.[44] Davidson and co-workers corroborated the high stability of the trimethylsilyl radical, generated by the pyrolysis of alkenyl- and *tert*-butylsilanes, by gas kinetic experiments.[45]

The presence of NH_3 is expected to partially inhibit the vinyl cross-linking process by competing for the free-radical sites produced by polysilane chain scission and vinyl coupling. In this manner, NH_3 could act as a "radical sink" by reacting with radical species, such as a trimethylsilyl radical, to produce an amine radical and a silane (or alkane):

$$NH_3 \xrightarrow{{}^\bullet Si\equiv \text{ (or } R^\bullet)} NH_2^\bullet + HSi\equiv \text{ (or RH)} \qquad (2)$$

The work of Fuyuki and co-workers[46] during the formation of silicon nitride thin films supports the formation of $NH_2^\bullet$ radicals by the reaction of NH_3 with silyl radicals. These workers detected $NH_2^\bullet$ radicals resulting from the 254-nm Hg photosensitization of SiH_4–NH_3 gas mixtures and photolysis of NH_3 at 185 nm. The dissociation of NH_3 and SiH_4 produced $H^\bullet$, $NH_2^\bullet$, and $SiH_3^\bullet$ radicals which reacted with the surface of the growing silicon nitride film.[46]

---

(41) Singer, L. S.; Lewis, I. C. *Appl. Spectrosc.* **1982**, *36*, 52–57.

(42) See for example: (a) O'Neal, H. E.; Ring, M. A. *Organometallics* **1988**, *7*, 1017. (b) Gano, D. R.; Gordon, M. S.; Boatz, J. A. *J. Am. Chem. Soc.* **1991**, *113*, 6711–6718. (c) Tang, Y.-N. In *Reactive Intermediates*; Abramovitch, R. A., Ed.; Plenum Press: New York, 1982; Vol. 2, Chapter 4, pp 297–366. (d) Wu, H.-J.; Interrante, L. V. *Macromolecules* **1992**, *25*, 1840–1841.

(43) Brix, T.; Bastian, E.; Potzinger, P. *J. Photochem. Photobiol., A:* **1989**, *49*, 287.

(44) Tokach, S. K.; Koob, R. D. *J. Phys. Chem.* **1980**, *84*, 1.

(45) (a) Davidson, I. M. T.; Barton, T. J.; Hughes, K. J.; Ijadi-Maghsoodi, S.; Revis, A.; Paul, G. C. *Organometallics* **1987**, *6*, 644–646. (b) Davidson, I. M. T.; Hughes, K. J.; Ijadi-Maghsoodi, S. *Organometallics* **1987**, *6*, 646–650.

(46) Fuyuki, T.; Allain, B.; Perrin, J. *J. Appl. Phys.* **1990**, *68*, 3322.

Reaction 2 could favor the formation of an open, porous network during thermal cross-linking of VPS by restricting the formation and condensation of a poly(carbosilane) network by capping dangling Si–CH$^\bullet$–CH$_2$R functionality. The differences in the morphology between samples 250A (Table I) and 250N[24] can be attributed to this effect. Each of the isolated, NH$_3$-pyrolyzed VPS samples was extensively macroporous, while VPS samples retrieved after identical heating schedules in N$_2$ were nonporous and smooth at the micrometer scale (Figure 2). This morphological difference was produced during the initial heating of the samples from 25 to 250 °C. Furthermore, the significantly higher specific surface area obtained for sample 1000A (ca. 220 m^2/g)[25] compared to that obtained for sample 1000N (less than 0.5 m^2/g) is consistent with the formation of a more open network structure in NH$_3$. The low level of nitrogen (0.31 wt %, Table II) found in sample 250A shows that the polysilane is also somewhat reactive toward NH$_3$ even at 250 °C.[29] In N$_2$ however, the radicals are not as easily quenched, and network formation through vinyl coupling and radical recombination is more extensive, leading to a smooth, nonporous sample morphology (Figure 2).

Pyrolysis in ammonia to 250 °C also significantly changes the local environment around the Si atoms (as seen by the large resonance envelope in the ^{29}Si solid state NMR spectrum, Figure 5b) such that a polysilane with different, well-resolved functional units, including poly(carbosilane) units, is not produced at 250 °C as it is in N$_2$.[24] Indeed, the solid-state ^{29}Si MAS NMR spectra of both 250A and 400A exhibit a significantly broader distribution of resonance frequencies than that of as-received VPS. Compared with the spectra of samples 250N and 400N,[24] these spectra (Figure 5b,c) suggest that in the presence of NH$_3$, the thermal degradation of the polysilane chain leads to a much wider distribution of Si microenvironments.

Direct evidence for radical quenching during NH$_3$ thermolysis is provided by the ESR measurements obtained for the 250A and 250N samples (Figure 6). Whereas samples heated in N$_2$ to 400 °C show appreciable spin densities, the samples heated in NH$_3$ to temperatures less than 500 °C exhibit spin densities which are below the level of detection for the method employed. The low spin densities observed for the samples pyrolyzed in NH$_3$ suggest that NH$_3$ competes effectively as a radical scavenger/quencher under the experimental conditions employed in this study.

Even at temperatures of 250 °C and below, initial reaction between the polysilane and NH$_3$ is apparently critical for complete conversion of VPS to Si$_3$N$_4$. Burns and Chandra[19a] reported the incorporation of significant amounts of excess C, based primarily on elemental analysis, in ceramics derived from the pyrolysis of various poly(carbosilane), methylchloropolysilane, and hydridopolysilazane precursors if cross-linking reactions were completed prior to further decomposition in NH$_3$. We have noted that excess C is retained in VPS samples which are first cross-linked by rapidly heating to 250 °C in N$_2$ prior to further heating to 1000 °C in NH$_3$. In contrast, no significant concentration of C remains if the VPS is crosslinked first in NH$_3$ flow below 250 °C, followed by further heating in NH$_3$ to 1000 °C.

Polymer Degradation. Major decomposition of the polysilane begins near 300 °C in either NH$_3$ or N$_2$ and continues to approximately 650 °C (Figure 1). Within this region of major weight loss, there is continued evolution of silyl fragments and low molecular weight oligomers, loss of –CH$_3$ moieties as methylsilanes and hydrocarbons, and incorporation of NH$_x$ species into the polymer backbone. Ammonia gas provides the source of N for insertion into the polysilane, acts as radical-transfer agent, and facilitates the loss of hydrocarbons. Thus, whereas the polymer forms a three-dimensional Si–C network upon pyrolysis in N$_2$, the C and H in the pendant functional groups are replaced by N–H$_x$ species, and an extended network containing Si–N bonds is formed by pyrolysis in NH$_3$.

Elemental analyses show that a significant level of N is incorporated into the preceramic polymer, from 3.9 wt % in sample 400A to 36.2 wt % in sample 650A. Simultaneously, the level of carbon has fallen from 43.2 wt % in sample 400A to 7.1 wt % in sample 650A. Gas analyses show significant levels of trimethylsilane, ethane, ethylene, methane, and tetramethylsilane. These results are in agreement with the observations of Burns and Chandra,[19a] which showed that the concentration of C significantly decreased, while that of N significantly increased, from 400 to 600 °C during their pyrolysis studies in NH$_3$. Seyferth and co-workers have reported that at temperatures greater than 400 °C, NH$_3$ causes the nucleophilic cleavage of the Si–C bonds in polysilazane polymers and methyl groups are lost as methane.[9g] The detection of methane in the present study is consistent with this description.

We attempted to determine whether amines were evolved during the decomposition of the polymer in NH$_3$; however, if present, these compounds were not resolved in the GC-IR study of the gases trapped during the pyrolysis. We presume that the formation of significant levels of amines is small, due in part to the continuous flow of NH$_3$ through the furnace tube (providing a high concentration of reactive gas in the reaction zone). The NH$_3$ would provide an ample supply of N and H and drive the preferential formation of hydrocarbons (while sweeping away product gases), especially in the presence of free radicals supplied, in part, from decomposition of the polysilane backbone.

Nitrogen can be incorporated into the polymeric network in several ways. One likely source of N is NH$_2^\bullet$ radicals which can be provided via NH$_3$-induced radical quenching reactions such as eq 2. During thermolysis, NH$_3$ or an NH$_2^\bullet$ radical could react directly with the polysilane backbone to displace alkane, silane, hydrogen, or a radical fragment:

$$\mathrm{NH_3} + {\equiv}\mathrm{Si{-}R} \rightarrow {\equiv}\mathrm{Si{-}NH_2} + \mathrm{RH} \qquad (\mathrm{R} = \mathrm{CH_3}, \mathrm{H}, \text{ or } \mathrm{Si}{\equiv}) \quad (3)$$

$$\mathrm{NH_2}^\bullet + {\equiv}\mathrm{Si{-}H}\ (\text{or } {\equiv}\mathrm{C{-}H}) \rightarrow \mathrm{NH_3} + {\equiv}\mathrm{Si}^\bullet\ (\text{or } {\equiv}\mathrm{C}^\bullet) \qquad (\text{propagation}) \quad (4)$$

$$\mathrm{NH_2}^\bullet + {\equiv}\mathrm{Si}^\bullet \rightarrow {\equiv}\mathrm{Si{-}NH_2}\ (\text{termination}) \quad (5)$$

Similarly, reactions involving polymer-based radicals and NH$_3$ could also serve to introduce SiNH$_2$ groups, i.e.

$$\mathrm{NH_3} + {\equiv}\mathrm{Si}^\bullet \rightarrow \mathrm{H_2N{-}Si}{\equiv} + \mathrm{H}^\bullet \quad (6)$$

The H$^\bullet$ radicals could then, in turn, produce NH$_2^\bullet$ radicals by reaction with NH$_3$:

$$\mathrm{H}^\bullet + \mathrm{NH_3} \rightarrow \mathrm{NH_2}^\bullet + \mathrm{H_2} \quad (7)$$

Ammonia could also react directly with silylene species, which would insert into the N–H bonds:

$$\mathrm{NH_3} + {:}\mathrm{Si}{=} \rightarrow \mathrm{H_2N{-}Si(H)}{=} \quad (8)$$

The silyl amines so generated could then go on to eliminate NH$_3$ in thermally induced condensation/transamination reactions, producing silazanes, as has been suggested for polycarbosilazanes:[47]

$$2 \equiv\!Si{-}NH_2 \rightarrow \equiv\!Si{-}NH{-}Si\!\equiv + NH_3 \tag{9}$$

At higher temperatures, these silazanes would eventually go on to form Si_3N_4:

$$\equiv\!Si{-}NH_2 + \equiv\!Si{-}NH{-}Si\!\equiv \rightarrow (\equiv\!Si)_3N + NH_3 \tag{10}$$

The incorporation of N into the polymer, coupled with the loss of C, is most directly evidenced by the elemental analysis of the isolated solid pyrolysis products (Table II). Further evidence is provided by the associated infrared spectra (Figure 3). The IR spectrum of sample 400A (Figure 3c) shows a small increase in the intensity of the N–H stretch and the C–H stretching bands have lost resolution, relative to the spectrum of sample 250A. The 400A spectrum shows a relative increase in the intensity of the Si–H stretch, suggesting that the incorporation of N produces additional Si–H functionality.

Solid-state ^{13}C and ^{29}Si NMR spectra of sample 400A also show changes relative to the corresponding spectra of the 250A sample. By 400 °C, the number of different C environments has increased as seen by the broadened peak in the ^{13}C spectrum (Figure 4c). The ^{29}Si spectrum of sample 400A also appears to shift to lower shielding, possibly reflecting increased nitrogen substitution at the Si nucleus.

In addition to the silylamine condensation process noted above (eq 9), these experimental observations could be explained using an imine insertion mechanism analogous to the methylene (silylene) insertion reaction for polysilanes, which in this case converts the polysilane backbone with pendant amine groups to a polysilazane (eqs 11 and 12, where $R^\bullet = H^\bullet, NH_2^\bullet$, or $\equiv\!Si^*$).

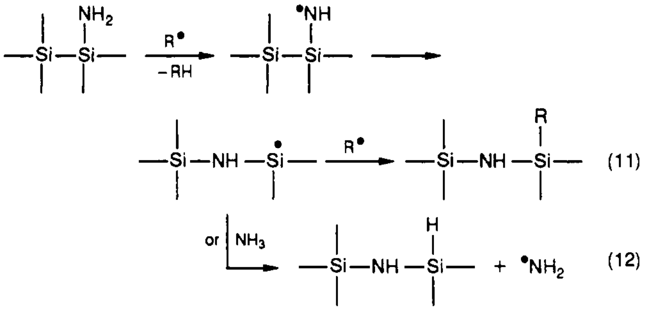

The occurrence of this type of reaction is supported by the relatively large intensity of the Si–H infrared stretch for samples 400A and 650A (Figure 3). Free-radical species are quenched in this reaction, which may cause both the observed plateau in the spin density concentration between 650 and 825 °C, and the decrease in the spin density concentration at higher temperatures for the NH_3-pyrolyzed samples (Figure 6).

Following pyrolysis in NH_3 to 650 °C, an appreciable amount of N has been incorporated into the preceramic VPS, as evidenced by the increase in the intensity of the N–H and Si–N stretching bands in the IR spectrum (sample 650A) along with significant loss of C–H intensity and broadening of the Si–H band. The loss of C-containing species is also apparent from the solid-state ^{13}C MAS NMR spectrum of sample 650A, which shows essentially no C–H functionality, and the ^{29}Si NMR spectrum, which shows a single, broad band (but narrow relative to the spectrum of sample 400A) indicative of predominantly SiN_4 environments.[39,40] Taki and co-workers[18b] also noted a similar loss of intensity corresponding to the ^{29}Si–C bond resonance and an increase in the intensity of the ^{29}Si–N resonance, beginning near 500 °C, and completed between 800 and 1000 °C for a poly(carbosilane) heated in NH_3. Their solid-state ^{13}C spectra showed complete loss of carbon by 700 °C.

It seems likely that the incorporation of N during the conversion of VPS to Si_3N_4 is dependent on the interaction of NH_3 with the porous sample morphology that is formed during cross-linking of the polymer, i.e., radicals generated in the decomposing polymer can generate $NH_2^\bullet$ radicals which can insert N directly. The efficient removal of gaseous byproducts would also be promoted by the corresponding high surface area to volume ratio.

Heterogeneous decomposition of NH_3 from 700 to 900 °C is reportedly accelerated by increased surface area and pore volume of silica/quartz fibers.[48] These researchers concluded that the decomposition reaction occurs within the pores of the glass and that the rate of the reaction is limited by both the rates of diffusion of NH_3 into the pores and diffusion of reaction products out of the pores. The work of Schroeder and Jarek[49] and recently by Lednor and co-workers[50] also suggests that the incorporation of significant levels of nitrogen from the decomposition of NH_3 requires a relatively small particle size (high surface area). These types of reactions probably involve radical sites on the surface of the Si-containing material, in a manner quite analogous to that which occurs during the pyrolysis of VPS in NH_3. Clearly, the high surface area of these samples promotes the efficient diffusion of NH_3 into close proximity with the converting polysilane network. Following diffusion of NH_3 into a pore within the network, the NH_3 can react with the surface of the preceramic solid. As a result of the reaction, the gaseous alkane and silane byproducts would diffuse out and leave behind a pitted region on the surface. This pitted region increases both the surface area and thus, the reactivity of the converting solid toward ammonia.

Van Dijen and Pluijmakers recently discussed the efficacy of NH_3 for removing carbon from SiC and Si_3N_4 ceramic powders as well as the dissociation of NH_3.[51] They noted that the heterogeneous dissociation of NH_3

$$2NH_3 \rightarrow N_2 + 3H_2 \tag{13}$$

depends strongly on the reactivity of the surface involved, and requires temperatures at least as high as 300 °C. Equation 13 is thermodynamically favored[51] over the formation of HCN from residual C according to the reaction

$$C + NH_3 \rightarrow HCN + H_2 \tag{14}$$

However, the latter reaction proceeds to a significant extent at temperatures above 700 °C, so that under these conditions, both the dissociation of NH_3 and the loss of excess carbon as HCN occur simultaneously.

In recent studies on the decomposition of Yajima's poly(carbosilane) in NH_3, it was found that the dissociation of NH_3 is negligible below 650 °C.[22] In the current study of the conversion of VPS in NH_3, the major increase in weight percent N and the decrease in weight percent C occurs between 400 and 650 °C (Table II). These temperatures are well below those required for either the production of HCN (eq 14) as a major route for carbon loss,

---

[47] Bacque, E.; Pillot, J.-P.; Birot, M.; Dunogues, J.; Lapouyade, P.; Bouillon, E.; Pailler, R. *Chem. Mater.* **1991**, *3*, 348–355.

[48] Bodenstien, M.; Kranendieck, F. *Nernst's Festschrift* (*Halle, 1912*) 99; *Chem. Abstr.* **1913**, *7*, 1647.

[49] Schroeder, J.; Jarek, J. J. *J. Non-Cryst. Solids* **1988**, *102*, 181–195.

[50] (a) Lednor, P. W.; de Ruiter, R. *J. Chem. Soc., Chem. Commun.* **1989**, 320–321. (b) Chorley, R. W.; Lednor, P. W. *Adv. Mater.* **1991**, *3*, 474–485.

[51] Van Dijen, F. K.; Pluijmakers, J. *J. Eur. Ceram. Soc.* **1989**, *5*, 385–390 and references therein.

or the significant dissociation of NH_3. Thus, our results suggest that the main processes which incorporate N during the conversion of the vinylic polysilane to Si_3N_4 do not involve intermediate species which are generated during the thermal decomposition of NH_3. This conclusion supports the earlier observations by Corriu et al. for the Yajima poly(carbosilane).[22]

The observed reduction in weight percent C between samples 650A (7.10% C) and 1000A (1.79% C, Table II) shows that at temperatures greater than 650 °C, NH_3 can effectively remove residual "free" carbon, which is present as CH_n species based on solid-state NMR studies, from the VPS pyrolysis product, probably by reactions such as eq 14.

Crystallization of VPS to α-Si_3N_4. At temperatures greater than 650 °C, the preceramic Si_xN_y material derived from the pyrolysis of VPS in NH_3 continues to lose nearly all of the remaining C and begins to crystallize. Sample 1000A is amorphous by X-ray powder diffraction,[25] has a high specific surface area, and contains a considerable amount of H, presumably as $=NH$ and $-NH_2$ residue, as seen in the IR spectrum. Transmission electron microscopy, combined with selected area diffraction techniques, confirms that sample 1000A actually contains homogeneously dispersed, nanometer-sized crystals of α-Si_3N_4.[25]

With increased heating of the 1000A samples in N_2 to 1600 °C, residual H is lost and the NH_3-pyrolyzed VPS ceramic crystallizes to predominantly α-Si_3N_4. The amorphous-to-crystalline phase transformation is confirmed by the sharpening of the single peak in the ^{29}Si MAS NMR spectra (Figure 5d–f), the sharpening of the bands specific for α-Si_3N_4 in the IR spectrum,[25] the sharpened X-ray diffraction patterns,[25] and the 10-fold decrease in specific surface area with increased temperature.[25] Unlike the crystallization of sample 1000N (from the analogous N_2 pyrolysis),[24] grain growth occurs readily in sample 1000A. In the former case, grain growth is most likely hindered by the presence of finely dispersed graphitic C, which is probably concentrated along the crystal grain boundaries.

ESR and DNP Analysis. From the data reported in Table III, it can be seen that the ^{13}C NMR intensity in the NH_3-pyrolyzed sample 650A shows enhancement only at the positive and negative solid-state condition, which implies that the free radicals are stationary, e.g., centered on broken bonds.[52] The solid-state effect depends on static interactions between nuclear spins and the unpaired electrons; the manifestation of this mechanism indicates the presence of fixed paramagnetic centers.[52]

The N_2-pyrolyzed sample 650N, in contrast, shows an enhancement under each of the solid-state, Overhauser, and thermal mixing conditions, which suggests that there is both a mobile and a stationary component to the population of free radicals in the sample. The Overhauser effect depends upon time-dependent interactions between nuclear spins and the unpaired electrons with substantial frequency components at the electron-spin Larmor frequency (39.5 gHz in the present case); the manifestation of this mechanism indicates mobile unpaired electrons or free-radical moieties in rapid motion.[52] The Overhauser characteristic could be attributed to the large graphitic regions in sample 650N,[24] which are likely to contain mobile electrons, whereas the solid-state effect could come about from stationary unpaired electrons centered on broken bonds. The thermal mixing effect relies on strong dipole interactions between unpaired electrons and requires high concentrations of paramagnetic centers.

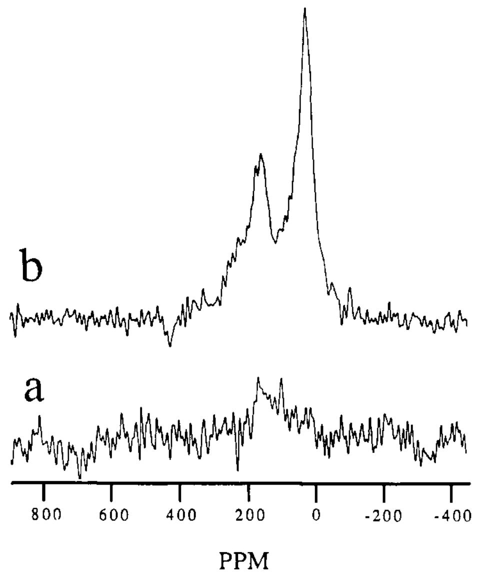

Figure 8. Natural-abundance 15.0-MHz solid-state ^{13}C NMR spectra of sample 650N (obtained from the pyrolysis of VPS in N_2[24]) showing the effect of DNP enhancement: (a) normal Bloch decay spectrum without DNP enhancement; (b) spectrum incorporating DNP enhancement at the positive solid-state condition for ^{13}C.

Since each effect is significantly enhanced for sample 650N, we conclude that a high concentration of free radicals and paramagnetic centers exist in this sample. In contrast, the effects are quite minimal in sample 650A, which must be attributed to the role that NH_3 performs in quenching free-radical sites during pyrolysis.

The DNP results imply that the distribution of free radicals in the NH_3-pyrolyzed samples is more homogeneous than analogous samples prepared by N_2 pyrolysis at a temperature of 650 °C. To demonstrate the DNP enhancement, two solid-state ^{13}C spectra were obtained for sample 650N. One consisted of a typical Bloch decay spectrum without DNP enhancement (Figure 8a). The second spectrum incorporated DNP enhancement at the positive solid state condition for carbon-13 (Figure 8b). The two peaks observed in the latter spectrum have the same respective chemical shifts as the graphitic and carbidic carbons in the previously assigned solid-state NMR spectra of sample 650N.[24]

Conclusions

The use of NH_3 gas during the pyrolysis of a vinylic polysilane to 1000 °C produces silicon nitride, while the use of N_2 produces C-rich silicon carbide. At temperatures as high as 300 °C, cross-linking of the vinyl groups and partial decomposition of the polymer proceeds in NH_3 essentially as it does in N_2. Some hydrosilylation also occurs by reaction of hydrido groups with vinyl groups. NH_3 produces a macroscopically porous sample at this temperature, implying that there is chemical interaction of this gas with the polysilane during cross-linking.

The major differences in chemistry due to pyrolysis atmosphere are seen from 300 to 650 °C, where the largest weight loss occurs. Within this temperature range, there is substantial cleavage of the polysilane backbone and significant methylene insertion which causes additional Si–H bonds to form. Also occurring in this temperature range is the NH_3-assisted elimination of hydrocarbons and the replacement of Si–C bonds by Si–N bonds, which eventually converts the polysilane backbone to that of a

---

(52) Wind, R. A.; Duijvestijn, M. J.; Van Der Lugt, C.; Manenschun, A.; Vriend, J. In *Progress in NMR Spectroscopy*; Pergamon Press: New York, 1985; Vol. 17, pp 33–67.

polysilazane. The efficient removal of C in the polymer by NH_3 produces a homogeneous distribution of stationary radical sites in the polymer. In contrast, graphite-rich regions containing mobile electrons are produced by the N_2 pyrolysis. Heating to temperatures as high as 1000 °C in NH_3, and to higher temperatures in N_2, causes both the loss of residual C and H and eventual crystallization of the amorphous Si_xN_y network to α-Si_3N_4.

Although the thermally induced dissociation of NH_3 is negligible below 650 °C, we observe significant N levels in the ceramic product isolated at 400 °C. This result implies that NH_3 is not thermally dissociated prior to reaction with the polysilane backbone. Our ESR results suggest that free radical sites produced at relatively low temperatures by decomposition of the polymer are scavenged by the NH_3 pyrolysis gas. NH_3 then serves as a radical transfer agent which can generate species that can subsequently react with the polymer to incorporate N.

Acknowledgment. The National Science Foundation is acknowledged for support under Materials Chemistry Initiative Grant No. CHE-8706131, along with the Colorado State University NMR Center, funded under NSF Grant No. CHE-8616437.

Nonlinear Optical Properties of Magnetically Aligned Solid Solutions of Nematic Polymers and Dye Molecules

S. I. Stupp,[*,†,‡,§] H. C. Lin,[†,‡] and D. R. Wake[‡]

Department of Materials Science and Engineering, Materials Research Laboratory, and Beckman Institute for Advanced Science and Technology, University of Illinois at Urbana—Champaign, Urbana, Illinois 61801

Received November 5, 1991. Revised Manuscript Received May 27, 1992

We have studied the second-order nonlinear optical response of a solidified nematic polymer containing a photoactive organic dye as a dissolved solute or as phase-separated crystals. Solvation of the dye in the main-chain nematic is evidenced by melting point depression with increasing dye concentration up to 20% by weight. Electrical poling of the dye–polymer alloy below the melting point of the nematic host results in strong second harmonic intensities from an infrared laser pulse passing through the medium. A comparison of thermally stimulated discharge spectra of poled alloys with nonlinear optical measurements indicates that dipolar ordering of solute molecules in the electric field gives rise to second harmonic activity. Interestingly, magnetically induced order in the nematic solvent can result in second harmonic signals which are 6–9 times more intense, equivalent to the second-order susceptibility of the system tripling. In this macroscopically organized environment, polar ordering of the dye solute in the electric field occurs more rapidly than in the polydomain nematic phase. Furthermore, the thermal stability of the polar dye network is greater as well in the aligned environment. The magnetically aligned nematic alloy can be regarded as an "Ising-like" medium in which the nematic and the magnetic fields confine dipolar dye molecules along directions parallel or antiparallel to the applied electric field. Previous calculations predict an increase of the second-order susceptibility by a factor of 5 in an idealized system as compared to a factor of 3 found in these experiments.

Introduction

In recent years there has been rising interest in the field of nonlinear optical properties of organic solids. This statement is supported by many contributions to the literature, including reviews on the subject.[1,2] One of the specific properties of interest has been second harmonic generation (SHG), that is, doubling of the frequency of laser beams as they pass through organic media. Provided various technical difficulties are solved, some are of the opinion that the nonlinear optical properties of organic materials may be useful in electrooptical technologies that transmit or store information through light beams. It is well-known that SHG-active organic materials contain molecules with strong electron donor and acceptor groups separated by conjugated bonds.[3] Many if not most of these photoactive molecules are therefore dyes that have a large dipole moment along their principal axis. The medium which doubles the frequency must also be noncentrosymmetric, implying the organic material must be a single crystal lacking an inversion center or a matrix in which an external electric field has been used to bias the spatial orientation of the molecular dipoles and thus to break the inversion symmetry.

This paper studies a noncentrosymmetric medium for SHG formed by polymers with nematogenic backbones as a solvent for photoactive dye solutes. We reported recently our initial results on the system.[4] The physical idea is to produce an "Ising-like" solution of nematic polymer and dye in an external magnetic field in order to generate a macroscopic director but with random up or down dipolar orientation. If dye molecules tend to align with the solvent's backbone and the magnetic field defines a macroscopic director, then the local symmetry of the polymeric

---

[†] Department of Materials Science and Engineering.

[‡] Materials Research Laboratory.

[§] Beckman Institute for Advanced Science and Technology.

(1) Ulrich, D. R. In *Organic Materials for Nonlinear Optics*; Hann, R. A., Bloor, D., Eds.; Royal Society of Chemistry: London, 1989; p 241.

(2) *Nonlinear Optical Properties of Organic Molecules and Crystals*; Chemla, D. S., Zyss, J., Eds.; Academic Press: New York, 1987; Vols. I and II.

(3) Nicoud, J. F.; Twieg, R. J. In *Nonlinear Optical Properties of Organic Molecules and Crystals*; Chemla, D. S., Zyss, J., Eds.; Academic Press: New York, 1987; p 227.

(4) Lin, H. C.; Wake, D.; Stupp, S. I. *Bull. Am. Phys. Soc.* **1990**, *35*, 560.

0897-4756/92/2804-0947$03.00/0